

Seamless short- to mid-term probabilistic wind power forecasting

Gabriel Dantas^{a,*}, Jethro Browell^a

^a*School of Mathematics and Statistics, University of Glasgow, 132 University Pl, Glasgow, G12 8TA, UK*

Abstract

This paper presents a method for probabilistic wind power forecasting that quantifies and integrates uncertainties from weather forecasts and weather-to-power conversion. By addressing both uncertainty sources, the method achieves state-of-the-art results for lead times of 6 to 162 hours, eliminating the need for separate models for short- and mid-term forecasting. It also improves short-term forecasts during high weather uncertainty periods, which methods based on deterministic weather forecasts fail to capture. The study reveals that weather-to-power uncertainty is more significant for short-term forecasts, while weather forecast uncertainty dominates mid-term forecasts, with the transition point varying between wind farms. Offshore farms typically see this shift at shorter lead times than onshore ones. The findings are supported by an extensive, reproducible case study comprising 73 wind farms in Great Britain over five years.

Keywords: Wind energy, forecasting, probabilistic, uncertainty, weather predictions

*Corresponding author

Acronyms

BAV	Bid Acceptance Volume.
BMA	Bayesian Model Averaging.
BMRA	Balancing Mechanism Reporting Agent.
CDF	Cumulative Distribution Function.
CRPS	Continuous Ranked Probability Score.
EMOS	Ensemble Model Output Statistics.
GBT	Gradient Boosting Trees.
GPD	Generalized Pareto Distribution.
ML	Machine Learning.
NWP	Numerical Weather Prediction.
PDF	Probability Density Function.
TSO	Transmission System Operator.
WTG	Wind Turbine Generator.

1. Introduction

Wind power is a key technology in low-carbon power systems [1, 2]; however, high penetration of wind power presents significant operational challenges for electricity markets and networks [3, 4, 5, 6, 7]. Electricity markets and networks were designed for dispatchable generation [4], but wind power production is stochastic and intermittent with limited predictability. In this context, wind power forecasting from six hours to seven days ahead is essential for the economic and reliable integration of wind energy into existing markets and networks [8, 9, 10, 11, 12]. Forecast information for horizons up to forty-eight hours ahead directly influences decisions made by Transmission System Operators (TSOs), such as unit commitment, congestion management, and scheduling storage in addition to decisions related to energy trading in day-ahead and intraday markets [11, 8]. Forecasts from two to

seven days ahead influence operational planning and maintenance scheduling [13].

Historically, network operation and market participation have been based on single-point forecasts, i.e., based exclusively on the expected value of the energy generation/demand. However, the way forecast information is used is evolving. Probabilistic forecasts are increasingly utilised directly via visualisation as well as in forecast-based decision-support and automation [14, 8]. Probabilistic forecasting is attractive because it provides information about the expected value plus associated forecast uncertainty.

The methods employed in wind power forecasting intrinsically relate to the time scale of interest. Probabilistic wind power forecasting targeting very short-term horizons (up to six hours ahead) is characterised by time series-based methods [15, 16, 17]. However, the performance of time series-based models degrades rapidly for longer horizons. Therefore, for horizons from six hours to seven days ahead, it is necessary to use Numerical Weather Prediction (NWP) as inputs to statistical and machine learning (ML) models.

NWP models forecast atmospheric behaviour by numerically solving a system of non-linear differential equations that describe physical processes after first estimating the current state of the atmosphere. The errors associated with NWP models are caused by inaccuracies related to subgrid dynamical and physical processes, as well as errors associated with initial and boundary conditions [18]. Understanding such errors is fundamental to interpreting NWP, as the atmosphere is a chaotic system. Thus, ensemble NWP models, which produce multiple distinct forecast scenarios based on perturbed initial conditions and model physics, have been developed to quantify NWP uncertainty.

NWP-based wind power forecasting may be separated into two main tasks. The first involves correcting the NWP to obtain a more reliable and accurate description of the atmospheric variables at the location of interest. This correction is necessary, as the NWP model’s intrinsic errors usually culminate in biased and underdispersed predictions when compared to observations made at a particular location [19, 20]. The second task is associated with modelling the relationship between atmospheric variables predicted by the NWP model and the wind farm’s power output (here, called the weather-to-power relationship¹).

¹The terms wind-to-power [21], power curve [22], or simply forecasting model [19] are

NWP-based methods are used to forecast output wind power for a wide range of horizons with strong use-cases for TSOs and energy markets from six-hours to seven-days ahead. Usually, these forecast horizons are subdivided into short- or mid-term, where users reasonably expect different levels of forecast performance. However, the wind power forecasting literature lacks a well-defined threshold between these time scales. Furthermore, while there is an emerging consensus on state-of-the-art methods for short-term forecasting, this is lacking for mid-term. Thus, in many cases, classification developed within the scope of wind speed forecasting is used.

While the classification of NWP-based forecasting methodologies according to short- and mid-term is not well defined, the type of information provided by the NWP model is a differentiating characteristic related to forecast horizon. NWP-based methodologies can be classified by being based on deterministic or ensemble NWP models. Deterministic NWP models provide a single-valued forecast of an atmospheric quantity at a specific location. On the other hand, ensemble NWP models run many similar but not identical versions of the NWP model in parallel (e.g., different initial conditions and model parameterisations). Therefore, ensemble NWP models provide multiple scenarios for the same atmospheric quantity and location, allowing the quantification of NWP model uncertainty [18].

The following sub-sections summarise the state-of-the-art NWP-based probabilistic wind power forecasting methodologies powered by deterministic NWP and ensemble NWP, respectively. Finally, we present the contributions of this work.

1.1. Methodologies based on deterministic NWP

Short-term wind power forecasting methodologies based on deterministic NWP are not provided with direct quantification of weather forecast uncertainty. Thus, all uncertainty estimation is performed by post-processing. These methods do not differentiate between NWP bias correction and weather-to-power modelling: statistical or ML models directly predict wind farm power output from deterministic NWP model outputs.

The statistical and ML models employed by these methodologies can be divided into models that produce parametric or non-parametric density

usually used in the literature related to wind power forecasting. However, this work uses the term weather-to-power to emphasise that atmospheric variables other than wind speed are commonly used as input for this modelling task.

forecasts. Parametric forecasts assume that the distribution of the predicted wind power at a given time follows a given probability distribution, e.g. Beta, see for example Lange [23], Bludszuweit et al. [24], Pinson [25], Bremnes [26], Messner et al. [27]. In general, parametric methods are less computationally demanding than non-parametric. However, the use of parametric forecasts has limitations. First, the challenge related to choosing a family of appropriate distributions to describe wind power generation. Furthermore, due to the complexity of wind power production, the family of distributions that best describes wind power can change over time and between wind farms. Therefore, parametric forecasts are restrictive and may be too inflexible to produce accurate forecasts in many settings [14].

As a result, non-parametric wind power forecasting methodologies have been established as best-in-class in recent literature and forecasting competitions for horizons up to two days-ahead [28, 14, 8]. These include linear quantile regression (e.g., Juban et al. [29]); gradient boosting trees (GBT - e.g., Andrade and Bessa [30], Nagy et al. [31], and Landry et al. [32]); kernel density estimation (e.g., Guan et al. [33], Juban et al. [34], Zhang and Wang [35], Dong et al. [36], Bessa et al. [37]), and analogues (e.g., Junk et al. [38], Alessandrini et al. [39], Shahriari et al. [40], Mangalova and Shesterneva [41], Zhang and Wang [35]). In addition, many of the methods proposed in the recent literature use feature engineering to pre-process NWP model outputs to extract temporal information, spatial information, or both, from multi-dimensional NWP data (e.g., Andrade and Bessa [30], Juban et al. [29], Nagy et al. [31]). Feature engineering plays a crucial role in maximising performance, as evidenced in forecast competitions. Results indicate that feature engineering can impact forecast performance as much as the choice of statistical/ML model [28, 30].

1.2. Methodologies based on ensemble NWP

Ensemble NWP models provide multiple scenarios for the same atmospheric quantity in a specific spatial position called ensemble members. Thus, they allow the estimation of weather forecast uncertainty as well as the most likely outcome [18]. The literature on methodologies that leverage ensemble NWP is much smaller than that of deterministic NWP. The limited number of related works is perhaps due to the size, complexity and accessibility of ensemble datasets, though these barriers are reducing. Furthermore, most evaluate overall forecast performance in terms of average metrics and overlook the potential of ensemble information in high-impact situations, such as

periods of high weather uncertainty, as we explore in Section 4.3.

Forecasting methods based on ensemble NWP can be classified according to the number of stages used to model the target, i.e., single- and dual-stage methodologies. In dual-stage methodologies, one stage is dedicated to weather-to-power modelling and the other to post-processing the resulting ensemble of power forecasts. Using a dedicated weather-to-power model allows dual-stage methodologies to use established ensemble post-processing methods in the second stage to produce the final wind power forecast. Models originally proposed for atmospheric variables are generally unable to explain the non-linear, bounded, weather-to-power relationship skillfully. Single-stage methodologies use only one stage to forecast the output wind power based on the information in the NWP ensemble.

Single-stage methodologies usually use more complex ML and statistical models than dual-stage ones. The models used in single-stage methodologies are often non-linear and provide less interpretability². Only a small number of studies propose single-stage methodologies. Among the main contributions are Wu et al. [43], proposing Lower Upper Bound Estimation with shallow neural networks, Zhang et al. [44] proposed a deep learning framework based on a multi-source temporal attention network; and Fujimoto et al. [45] proposed using natural gradient boosting for probability density prediction. However, they are all complex methods that demand high computational effort and allow low interpretability. Furthermore, some do not follow best practices for forecast evaluation, restricting their informativeness.

Regarding dual-stage methodologies, the stage related to weather-to-power modelling is usually performed by statistical and ML models. The models used to describe the weather-to-power relationship can be linear (e.g., polynomial regression [46], segmented linear regression [22, 19]) or non-linear (e.g., logistic regression [47], artificial neural networks [48, 19], and random forests [19]). The stage related to ensemble calibration generally uses statistical models originally proposed to forecast atmospheric variables.

Statistical models used in this context are typically easy to implement, require low computational effort and are relatively interpretable. The most prominent statistical models used for ensemble calibration are Bayesian Model

²Interpretability can be understood in this context as “the degree to which an observer can understand the cause of a decision” [42]

Averaging (BMA) (e.g., [22]) and Ensemble Model Output Statistics (EMOS)³ [49] (e.g., [19]). BMA was originally proposed in Raftery et al. [50] in order to re-calibrate ensemble forecasts. It can be understood as a mixture of parametric distributions, i.e., kernels. In BMA, each NWP model ensemble member is dressed with a probability distribution. The BMA coefficients control each kernel’s weight and variance and are estimated by maximising some likelihood. Therefore, BMA can be understood as a non-parametric model. On the other hand, EMOS, originally proposed in Gneiting et al. [51], is a parametric model widely used in the post-processing of NWP ensembles. EMOS aims to describe the posterior distribution parameters as functions of ensemble statistics (e.g., the average and standard deviation of ensemble members). Due to its computational simplicity and satisfactory results, EMOS is widely used in operational post-processing at weather services [19]. The preference for using EMOS also extends to the context of probabilistic wind power forecasting powered by ensemble NWP. The most commonly used distribution families in EMOS applications for wind power are Truncated Normal [19, 52] and Gamma [19]. Other models have been developed to calibrate ensembles to forecast atmospheric variables, e.g., member-by-member post-processing [53] and isotonic distributional regression [54]. However, they have yet to be widely explored in the context of wind power forecasting. Despite the growing literature associated with probabilistic weather-to-power modelling [55], dual-stage forecasting methodologies only adopted single-point models, to the best of the authors knowledge. Thus, methodologies powered by ensembleNWP proposed to date ignore a key source of uncertainty and naively attempt to account for it in ensemble post-processing.

1.3. Contributions

Methodologies based on deterministic NWP perform all uncertainty estimation through post-processing. Existing methodologies based on ensemble NWP either combine ensemble calibration with a deterministic weather-to-power model or forecast power production directly based on features derived from ensemble NWP. Existing methodologies do not distinguish between sources of uncertainty and implicitly attempt to correct this via post-processing. To the best of the authors’ knowledge, this work is the first to propose a method that explicitly models and combines NWP forecast uncer-

³EMOS is also referred to in the literature as nonhomogeneous regression.

tainty and uncertainty arising from weather-to-power conversion.

This work’s first contribution is a novel method for seamless short- to mid-term wind power forecasting based on probabilistic weather-to-power modelling ensemble post-processing. This method explicitly models and combines the uncertainties from NWP and the weather-to-power relationship. Through an extensive and fully reproducible case study, the proposed method is shown to have significant performance benefits.

The second contribution is a study of the relative performance of state-of-the-art methods based on deterministic and ensemble NWP, which is absent from the current literature.

Finally, the lead-time at which ensemble NWP adds benefit for wind power forecasting is investigated and shown to vary between wind farms; however, there is a clear difference between onshore and offshore wind farms in Great Britain.

The remainder of this work is organised as follows. Section 2 describes the proposed method and the state-of-the-art reference methodologies adopted to compare with the proposed method. Section 3 describes the NWP models and observational data sets. This work used five years of observational data from 73 wind farms in Great Britain and deterministic and ensemble NWP models provided by ECMWF. Section 4 presents and discusses the results. Section 5 addresses the conclusions and perspective regarding future works.

2. Methodology

The method proposed in this work is based on two stages. A probabilistic description of the weather-to-power relationship and the combination of the probabilistic weather-to-power model with the ensemble NWP. In the following text, $\hat{x}_{t+k|t}$ is the forecast of x_{t+k} produced using the NWP with base time t (i.e., horizon k steps ahead of the base time).

2.1. Probabilistic weather-to-power modelling

Weather-to-power relationship modelling aims to describe the wind farm’s output power given actual weather conditions as described by the NWP model to be used in forecasting. The weather-to-power relationship is uncertain, hence the probability distribution of power production is predicted given certain weather conditions.

Quantile regression with Gradient-Boosted Trees (GBT) is used to model the weather-to-power relationship, which is established as best-in-class for

similar tasks [30, 32, 56]. GBT are based on a non-parametric and non-linear ensemble learning algorithm. They can be understood as “an ensemble of weakly predictive regression trees, combined to generate a powerfully predictive collective” [57]. However, unlike models, such as random forests, which combine models in the ensemble via averaging, GBT is based on sequentially adding weak learners (i.e., regression trees) to the ensemble. A new base-learn is trained at each iteration, considering the error of the ensemble created so far. Furthermore, it is very flexible, accommodating a wide range of loss functions (though some implementations require a twice-differentiable loss, which excludes the standard quantile loss) and combinations of continuous and discrete features. See Friedman [58], Ke et al. [59] and Chen and Guestrin [60] for more details.

A separate GBT is estimated for each of the quantiles of interest. The GBT hyperparameters are tuned for each quantile using the Bayesian Optimization algorithm with random permutation cross-validation [61]. After choosing a set of hyperparameters, the GBT is estimated using all the data samples available for weather-to-power model estimation. As different GBTs are estimated for each quantile, it is not guaranteed that the predicted quantiles will be monotonically increasing (i.e., quantile crossing). Several strategies have been proposed to solve the quantile crossing problem [62, 63]. Here, quantiles are sorted to be monotonically increasing [29]. This strategy is adopted due to its simplicity and the satisfactory results achieved.

Weather-to-power modelling aims to predict the wind power given actual atmospheric conditions, as described by the NWP model. Therefore, the impact of NWP forecast uncertainty on the weather-to-power model estimate should be minimised. Therefore, only NWP operational analysis is used to fit GBTs. The ensemble NWP in this study provides equally likely future scenarios with no distinguishable features or ordering, i.e., exchangeable ensemble members. Exchangeability implies independence between forecasts performed at different base times. Therefore, estimating distinct predictive models for each ensemble member is not meaningful. Thus, the weather-to-power model is estimated using the ensemble median for each atmospheric variable and grid point. Note that the proposed method was developed for exchangeable ensemble members. However, if non-exchangeable ensembles are available, alternative treatments could be considered. In the following text, $\hat{q}_{j,t+k|t}^{(\tau)}$ is the quantile τ predicted by ensemble member j from the weather-to-power model.

2.2. Ensemble combination

The second stage of the proposed method incorporates weather forecast uncertainty using ensemble NWP. The ensemble captures weather forecast uncertainty, and each ensemble member is dressed with a kernel quantifying additional weather-to-power uncertainty for that ensemble member. The parameters of the kernels are derived from the probabilistic weather-to-power predictions described above. The mean of the j th kernel is given by the median of the weather-to-power predicted for ensemble member j at the corresponding time $t + k|t$

$$\hat{\mu}_{j,t+k|t} = \hat{q}_{j,t+k|t}^{(50)} \text{ for } j = 1, \dots, m \quad (1)$$

and the standard deviation is a linear function of the interquartile range (IQR)

$$\hat{\sigma}_{j,t+k|t} = \lambda_{0,k} + \lambda_{1,k} \left(\hat{q}_{j,t+k|t}^{(75)} - \hat{q}_{j,t+k|t}^{(25)} \right) \text{ for } j = 1, \dots, m \quad (2)$$

where $\lambda_{0,k} > 0$ and $\lambda_{1,k} \geq 0$ are the spread coefficients related to horizon k . The spread coefficients allow variation in the kernel dispersion over the forecast horizons. These variations are expected as the NWP accuracy tends to degrade as the forecast horizon increases, though this does not adjust the dispersion of the ensemble itself.

Using parametric kernels allows the Cumulative Distribution Function (CDF) associated with each ensemble member to be described by just three quantiles, significantly reducing computational effort compared to multiple quantile regression. In this work, the kernels follow a Normal distribution with CDF given by

$$\hat{F}_{j,t+k|t}(x) = \Phi \left(x; \hat{\mu}_{j,t+k|t}, \hat{\sigma}_{j,t+k|t} \right) \text{ for } j = 1, \dots, m \quad (3)$$

where $\hat{F}_{j,t+k|t}$ denotes the estimated CDF/kernel related to ensemble member j and Φ is the Normal CDF. The power data are non-negative, favouring the use of the Gamma distribution. However, both Gamma and Normal kernels produced almost identical results. Therefore, the Normal distribution was chosen for simplicity.

A beta-transformed linear opinion pool performs kernel combination to produce the final predictive density. Gneiting and Ranjan [64] proposed

the beta-transformed linear opinion pool to correct the miscalibration that typically results from simple linear combination due to dependency between kernels that, in many cases, is difficult to estimate. The CDF resulting from the kernel combination $\hat{G}_{j,t+k|t}$ at $x \in \mathbb{R}$ is given by

$$\hat{G}_{t+k|t}(x) = I_{a_k, b_k} \left(\frac{1}{m} \sum_{j=1}^m \hat{F}_{j,t+k|t}(x) \right) \quad (4)$$

$$I_{a_k, b_k}(z) = \frac{B_{a_k, b_k}(z)}{B_{a_k, b_k}}$$

where I_{a_k, b_k} denotes the CDF of the Beta density⁴ with parameters $a_k > 0$ and $b_k > 0$, and $B_{a_k, b_k}(z)$ and B_{a_k, b_k} are incomplete and complete beta functions, respectively.

Four coefficients describe the ensemble combination: two related to the ensemble spread correction, $\lambda_{0,k}$ and $\lambda_{1,k}$, and two associated with the beta-transformed linear opinion pool, a_k and b_k . Estimation is performed for each forecast horizon k by minimising a loss function ℓ that reflects forecast performance

$$\left[\hat{\lambda}_{0,k}, \hat{\lambda}_{1,k}, \hat{a}_k, \hat{b}_k \right] = \arg \min_{\lambda_{0,k}, \lambda_{1,k}, a_k, b_k} \ell(\lambda_{0,k}, \lambda_{1,k}, a_k, b_k) \quad . \quad (5)$$

The loss function used in this work is the mean Continuous Ranked Probability Score (CRPS). The CRPS is a strictly proper scoring rule widely used for evaluating probabilistic predictions [65]. It is recommended for probabilistic forecasting assessment because it reflects the paradigm of maximising the sharpness of the predictive distributions subject to calibration, though calibration should still be verified separately [66]. CRPS compares the predicted CDF \hat{F}_t on \mathbb{R} and the observation $y_t \in \mathbb{R}$. The mean CRPS is defined as

$$\ell(\hat{F}, y) = \frac{1}{n} \sum_{t=1}^n \int_{\mathbb{R}} \left(\hat{F}_t(x) - H(x - y_t) \right)^2 dx \quad (6)$$

where y_t is the observed value in t , \hat{F}_t is the predicted CDF that depends on

⁴The cumulative distribution function of the Beta density is also known as regularised incomplete beta function.

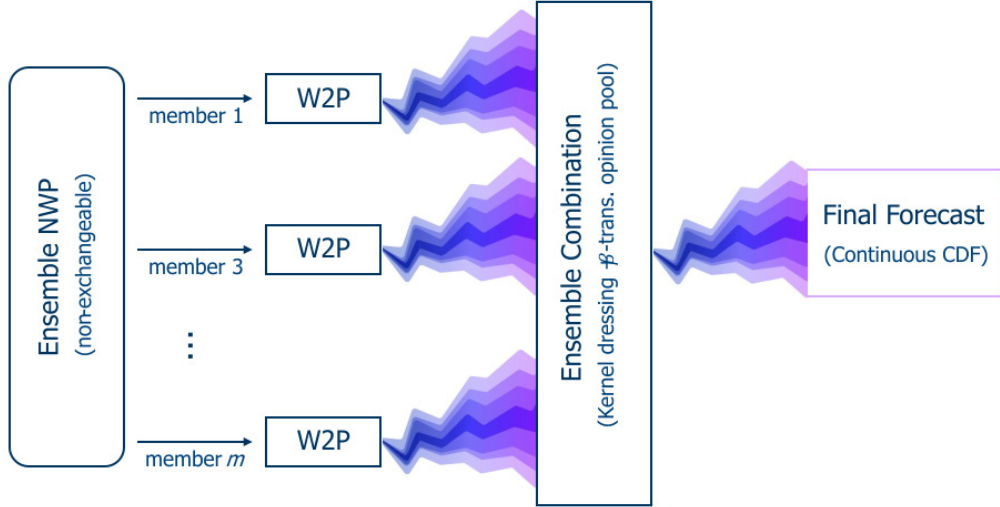


Figure 1: Diagram illustrating the proposed probabilistic wind power forecasting. Ensemble of numerical weather predictions are the input. Each ensemble member is converted into a probabilistic wind power prediction using a weather-to-power model. The resulting ensemble of power predictions are combined to produce the final probabilistic wind power forecast.

$\hat{\lambda}_0$, $\hat{\lambda}_1$, \hat{a}_k and \hat{b}_k , and $H(\cdot)$ is the Heaviside step function

$$H(z) = \begin{cases} 0 & \text{if } z < 0 \\ 1 & \text{if } z \geq 0 \end{cases} .$$

Figure 1 summarises the proposed method.

2.3. Reference methods

This work adopts four reference methods for two main reasons. First, to compare the proposed method with the established state-of-the-art. Second, to investigate the horizon where switching from deterministic to ensemble NWP adds values to the forecast, i.e., the threshold between short- and mid-term temporal scales. The following subsections present the reference methods, and Table 2 summarises their main characteristics. The reference methods are named according to the NWP model used as input, the weather-to-power model, and the ensemble combination/calibration model.

Table 2: Main characteristics of the reference methods and proposed method. Note that the method ENS-QGBT- β M refers to the proposed method.

Method	NWP model	Weather-to-power model	Calibration/ combination model	Tail model
ENS-GBT-None	Ensemble NWP (ECMWF-ENS)	Single-value GBT (i.e., \hat{q}_{50})	None	Peaks Over Thresholds
ENS-QGBT-None	Ensemble NWP (ECMWF-ENS)	Quantile GBT (see subsection 2.1)	None	Peaks Over Thresholds
HRES-QGBT-None	Deterministic NWP (ECMWF-HRES)	Quantile GBT originally proposed by Andrade and Bessa [30]	None	Peaks Over Thresholds
ENS-GBT-EMOS	Ensemble NWP (ECMWF-ENS)	Single-value GBT (i.e., \hat{q}_{50})	EMOS	None
ENS-QGBT- β M	Ensemble NWP (ECMWF-ENS)	Quantile GBT (see subsection 2.1)	Mixed model based on kernel dressing and beta-transformed linear opinion pool (see subsection 2.2)	None

2.3.1. ENS-GBT-None

The ENS-GBT-None is included as a benchmark. Each ensemble member is converted to power using the median provided by the weather-to-power model (i.e., $q^{(50)}$), no ensemble post-processing is performed before or after weather-to-power conversion. Density forecasts are constructed considering the ensemble members to be quantiles that are interpolated, and with a parametric tail distribution to extrapolate beyond the upper and lowermost quantiles. The parametric distribution used to model the tails is described in subsection 2.3.5.

2.3.2. ENS-QGBT-None

The ENS-QGBT-None is proposed here as the second benchmark. It aims to represent the accuracy obtained using a probabilistic weather-to-power model without performing ensemble correction or calibration. This method is fed by ensemble NWP. The weather-to-power model used by ENS-QGBT-None is the same as the method proposed in this work; however, no ensemble correction or calibration is performed. Thus, the final forecast is given by

$$\tilde{q}^{(\tau)} = \frac{1}{m} \sum_{j=1}^m \hat{q}_j^{(\tau)} \quad (7)$$

where $\tilde{q}^{(\tau)}$ is the final forecast for the quantile τ , and $\hat{q}_j^{(\tau)}$ is the quantile

τ estimated by the weather-to-power model using as input the ensemble member j .

2.3.3. *HRES-QGBT-None*

This reference method was originally proposed by Andrade and Bessa [30] and represents the state-of-the-art for short-term wind power forecasting. It was developed by improving the models that obtained first and second place in the Global Energy Forecasting Competition 2014 (GEFCom2014) [28], and Hybrid Energy Forecasting and Trading Competition 2024 [67].

This method is fed by a deterministic NWP model (in this case, ECMWF HRES) and produces non-parametric density forecasts. Feature engineering is used to extract spatial and temporal features from the gridded NWP data. For this method only, separate GBTs are estimated for each forecast horizon and quantile of interest. The hyperparameter tuning was also done separately for each forecast horizon and quantile using the Bayesian Optimization Algorithm [61].

2.3.4. *ENS-GBT-EMOS*

This reference method is based on the post-processing strategy that achieved the lowest CRPS in Phipps et al. [19]. This method represents the state-of-the-art probabilistic wind power forecasting based on ensemble NWP. It is a dual-stage method, where each NWP ensemble member is converted into wind power using a single-value weather-to-power model. The wind power ensemble is post-processed using EMOS to provide the final probabilistic wind power forecasting.

The weather-to-power model used by ENS-GBT-EMOS is the same as the proposed method. Therefore, it uses the same NWP input variables and horizontal domain. However, here, the weather-to-power model provides only single-value predictions.

EMOS performs ensemble combination on the ensemble of power forecasts. As discussed in subsection 1.2, EMOS is a parametric model widely used in post-processing NWP ensembles. EMOS estimates the parameters of the output density forecast as a function of the median and variance of the ensemble members. Gamma and Truncated Normal distribution families were initially tested, with Gamma achieving lower CRPS. Therefore, this reference method adopts the Gamma distribution. Thus, the parameters of the output density forecast are given by

$$\hat{\alpha}_{t+k|t} = \frac{\hat{\mu}_{t+k|t}^2}{\hat{\sigma}_{t+k|t}^2} \quad (8)$$

$$\hat{\beta}_{t+k|t} = \frac{\hat{\mu}_{t+k|t}}{\hat{\sigma}_{t+k|t}^2} \quad (9)$$

$$\hat{\mu}_{t+k|t} = c_{0,k} + c_{1,k} \overline{\hat{q}_{t+k|t}^{(50)}} \quad (10)$$

$$\hat{\sigma}_{t+k|t} = c_{2,k} + c_{3,k} \sigma_{\hat{q}_{t+k|t}^{(50)}} \quad (11)$$

where $\hat{\alpha}_{t+k|t}$ and $\hat{\beta}_{t+k|t}$ are the estimated shape and rate parameter of the Gamma distribution, respectively; $\hat{\mu}_{t+k|t}$ and $\hat{\sigma}_{t+k|t}$ are the estimated mean and standard deviation of the Gamma distribution; $c_{0,k}$, $c_{1,k}$, $c_{2,k}$ and $c_{3,k}$ are the EMOS coefficients; and $\overline{\hat{q}_{t+k|t}^{(50)}}$ and $\sigma_{\hat{q}_{t+k|t}^{(50)}}$ are the mean and standard deviation of the output power provided by the ensemble members, respectively. The EMOS coefficients are estimated by minimising the CRPS. For the EMOS coefficients estimation, this work utilises the CRPS closed form for Gamma distribution [68], given by

$$\begin{aligned} \text{CRPS}(F_{\mathcal{G}(\alpha,\beta)}, x) &= x (2F_{\mathcal{G}(\alpha,\beta)}(x) - 1) \\ &\quad - \frac{\alpha}{\beta} (2F_{\mathcal{G}(\alpha+1,\beta)}(x) - 1) \\ &\quad - \frac{\alpha}{\beta\pi} B\left(\alpha + \frac{1}{2}, \frac{1}{2}\right) \end{aligned} \quad (12)$$

where $F_{\mathcal{G}(\alpha,\beta)}$ is the CDF of the Gamma distribution with shape parameter α and rate parameter β , and B is the complete beta function. Note that the EMOS coefficients are estimated separately for each horizon k .

2.3.5. Distribution tails and quantiles of interest

The reference methods ENS-GBT-None, HRES-QGBT-None, and HRES-QGBT-None are non-parametric and provide quantiles as forecast output. The quantiles provided by these models range from 5% to 95% with 5% resolution (i.e., 19 quantiles). Methods based on non-parametric models

usually present difficulties in describing the tail of the predictive distribution. This difficulty stems from the need for a large volume of data to estimate sporadic events. Thus, this work adopts a hybrid approach using a parametric model to describe the distribution tails similarly to previous works [69, 70, 71, 72, 73]. The tails are modelled here using the Peak Over Threshold method [74], where the threshold exceedances follow the Generalized Pareto Distribution for sufficiently extreme thresholds. The Generalized Pareto Distribution (GPD) CDF is given by

$$\hat{D}_{t+k|t}(z_{t+k|t}; \hat{\eta}_k, \hat{\psi}_k, \hat{\xi}_k) = \begin{cases} 1 - \left(1 + \frac{\hat{\xi}_k(z_{t+k|t} - \hat{\eta}_k)}{\hat{\psi}_k}\right)^{-1/\hat{\xi}_k} & \text{for } \hat{\xi}_k \neq 0 \\ 1 - \exp\left(-\frac{\hat{\eta}_k - z_{t+k|t}}{\hat{\psi}_k}\right) & \text{for } \hat{\xi}_k = 0 \end{cases} \quad (13)$$

$$z_{t+k|t} = |x_{t+k} - \hat{e}_{t+k|t}|$$

in the above equations, \hat{D} is the estimated GPD's CDF, $z_{t+k|t}$ is the exceedance over the threshold $\hat{e}_{t+k|t}$, x_{t+k} is the output power at $t+k$; $\hat{\eta}_k, \hat{\psi}_k > 0$ and $\hat{\xi}_k$ are the location, scale and shape parameters estimated for the horizon k , respectively. Upper and lower tails can have different behaviours, so the GPD parameters are independently estimated by maximum likelihood. Here, the threshold for the lower tail is given by the predicted quantile 5% and the threshold for the upper tail is given by the predicted quantile 95%. The GPD is used in this work due to its flexibility, which allows the modelling of extreme events with light bounded tails when $\xi_k < 0$, heavy tails when $\xi_k > 0$, and exponential distribution when $\xi_k = 0$.

The forecast assessment performed in this work demands that forecast outputs be delivered as CDFs. Using CDFs in forecast assessment allows a consistent comparison between the different studied methods. Thus, the quantiles provided by the non-parametric reference methods are interpolated to obtain the predicted CDF. The interpolation is performed using the Piecewise Cubic Hermite Interpolating Polynomial algorithm [75] to preserve the monotonicity of the CDF.

The target variable studied in this work is the wind farm's metered energy output. The data were normalised by each wind farm's available capacity for ease of comparison between wind farms. Thus, the time series used in the context of this work are contained in a range [0,1]. However, the probabilistic forecasts performed by the reference methods are not necessarily constrained

to the unit interval. Thus, this work applied the solution proposed by Pinson [25]. This solution adds support (0,1) and probability masses on the boundaries 0 and 1. Thus, the predicted distributions become contained in the unit interval, maintaining the integral of the predicted PDF for $x \in [0, 1]$ equal to 1. The Probability Density Function (PDF) with probability masses on the boundaries is defined as

$$\hat{f}_{t+k|t}^*(x) = \omega_{0,t+k|t}\delta_0 + \hat{f}_{j,t+k|t}(x) + \omega_{1,t+k|t}\delta_1 \quad , \quad x \in [0, 1] \quad (14)$$

$$\omega_{0,t+k|t} = \hat{F}_{t+k|t}(x = 0)$$

$$\omega_{1,t+k|t} = 1 - \hat{F}_{t+k|t}(x = 1)$$

where $\hat{f}_{t+k|t}^*$ is the predicted PDF with probability masses on the boundaries; ω_0 and ω_1 are the weights related to the probability mass at 0 and 1, respectively; and δ_0 and δ_1 are Dirac delta functions at 0 and 1.

2.3.6. Assessment framework

This work uses CRPS, given by (6), to assess the performance of probabilistic forecasting methods. CRPS is a strictly proper scoring rule widely applied to evaluate probabilistic forecasting of continuous variables[76].

CRPS provides a general understanding of the predictive model's accuracy. Therefore, the attributes resulting from the CRPS decomposition — reliability and resolution — are used to assess specific aspects of the prediction [77, 78]. Reliability concerns the calibration of the forecasting model, i.e., whether the predicted probability agrees with the observed relative frequency. Reliability can be assessed through the value obtained from the CRPS decomposition as the resolution or visually through, for example, the reliability diagram [79]. Resolution concerns the ability of the forecasting model to discriminate between different outcomes of an observation.

This work also uses skill scores in order to compare the accuracy of distinct forecasting methods and the significance of any observed differences. The skill score S of the method s with respect to the method r for a performance metric A is given by

$$S_{r,s} = \frac{A_r - A_s}{A_r - A_{perf}} \quad (15)$$

where A_r is the metric value for the reference method, A_s is the metric value for the method of interest, and A_{perf} is the metric value for the ‘perfect’ prediction. $A_{perf} = 0$ for CRPS. Additionally, a bootstrap re-sampling of skill scores is used to determine if apparent differences in forecast accuracy (i.e., positive or negative skill score) differ significantly from the null hypothesis that skill is zero at the 0.05 level.

The predictive methods studied in this work vary significantly in handling the uncertainty associated with NWP and weather-to-power. Therefore, analysing the uncertainty associated with each process is necessary to understand predictive methods’ capabilities. The NWP uncertainty assesses the spread of the NWP ensemble. While the weather-to-power uncertainty is the average spread of the probabilistic power prediction across all ensemble members. Therefore the NWP uncertainty $U^{(NWP)}$ and the weather-to-power uncertainty $U^{(W2P)}$ are defined as

$$U_{t+k|t}^{(NWP)} = F_{75}^{-1} \left(\hat{q}_{j,t+k|t}^{(50)} \right) - F_{25}^{-1} \left(\hat{q}_{j,t+k|t}^{(50)} \right) \text{ for } j = 1, \dots, m \quad (16)$$

$$U_{t+k|t}^{(W2P)} = \frac{1}{m} \sum_{j=1}^m \left(\hat{q}_{j,t+k|t}^{(75)} - \hat{q}_{j,t+k|t}^{(25)} \right) \quad (17)$$

where F_{τ}^{-1} is the quantile function for probability τ , and $\hat{q}_j^{(25)}$, $\hat{q}_j^{(50)}$ and $\hat{q}_j^{(75)}$ are the quantiles 25%, 50% and 75% of the estimated output power related to the ensemble member j , respectively. Both uncertainty metrics consider the NWP converted into output power to provide a common framework for uncertainty assessment, facilitating comparison between them.

3. Case study

This section details the wind power and NWP datasets, model configurations, and cast study set-up used to evaluate and compare the abovementioned forecasting methods. All data, models and forecasts are shared along with this paper, as described in the Data Availability section.

3.1. Wind power data

In Great Britain (GB), the Balancing Mechanism Reporting Agent (BMRA) [80] is responsible for the settlement of the electricity market. Metered energy output and Bid Acceptance Volume (BAV) time series at 30-minute

intervals are used here. The BMRA database is subject to high standards imposed by the energy market [81].

Wind farms in GB are subject to curtailment. Curtailment can substantially modify the relationship between the weather patterns and the wind farm’s power output, significantly affecting forecasting systems [82, 83]. Estimated curtailment volumes are contained in BAV data. Thus, periods with non-zero BAVs were excluded from modelling and forecast evaluation.

The wind power time series were normalised by each wind farm’s available (or nominal) capacity to simplify the comparison of performance between wind farms of different capacities. Thus, the normalised time series have range [0,1]. However, the available capacity of wind farms can vary over time. The main reasons for this variation are the addition of new WTGs to the plant (i.e., during the construction phase) and the unavailability of WTGs or other electrical equipment due to outages and maintenance. The dataset provided by BMRA does not include information on the farms’ available capacity over time. Hence, the method described in the supplementary material was applied to estimate the available capacity at each time stamp (i.e., a time series of available capacity). Thus, this study assumes that the wind farm’s capacity is known at the time the forecast is produced.

Other measures were taken to increase the observational dataset’s reliability. The supplementary material discusses these measures in detail. As a result, some wind farms were completely excluded. Ultimately, 73 wind farms in Great Britain (34 onshore and 39 offshore) were retained. This study used data from 2019 to 2023. Figure 2 shows the location, nominal capacity, and type of the wind farms studied.

3.2. NWP data

The European Centre for Medium-Range Weather Forecasts (ECMWF) provides the deterministic and ensemble NWP models used in this work. The deterministic NWP is from the HRES model, and the ensemble NWP is from the ENS model. ENS model provides fifty exchangeable ensemble members. HRES was retrieved from the operational archive at full spatial and temporal resolution, but ENS dataset was retrieved from the TIGGE archive, which only stores a limited set of atmospheric variables at 6-hour/0.5° resolution. Retrieving multi-year full-resolution datasets of ENS from the operational archive is prohibitively slow and voluminous. Table 3 presents the main characteristics of the NWP models and the atmospheric variables used. The

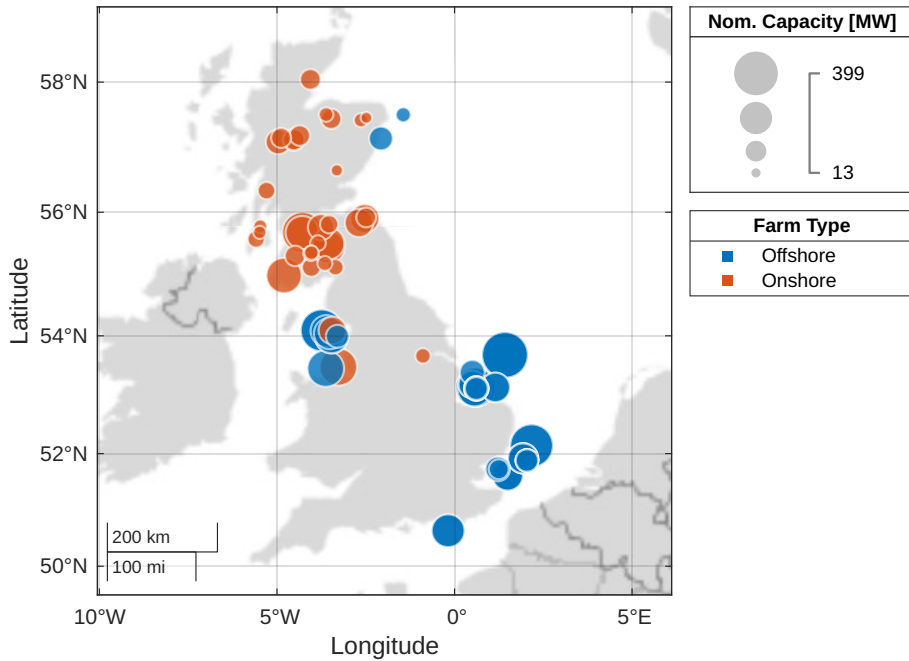


Figure 2: Map showing the wind farms included in the case study. Each wind farm is represented by a circle on the map. The circle’s diameter represents the wind farm’s nominal capacity, while the colour represents its type.

ENS model’s time step and computational effort required to perform the forecasts impose restrictions concerning the number of forecast horizons studied in this work. Thus, the forecast horizons studied in this work range from 6 hours to 168 hours ahead by 6-hour frequency.

3.3. Forecast model configurations

The method proposed in this work and the reference methods ENS-GBT-None, ENS-QGBT-None and ENS-GBT-EMOS use the same weather-to-power model described in subsection 2.1. Therefore, they all use exactly the same NWP data; see Table 4. The weather-to-power model is fed by six atmospheric variables from the four grid points closest to the wind farm of interest, totalling 24 inputs.

As discussed in subsection 2.1, the ideal scenario would use only NWP operational analysis and observational data to estimate the weather-to-power model. However, the operational analysis provided by the ensemble NWP dataset used in this work does not cover all hours of the day to be pre-

Table 3: List of main characteristics of the acquired NWP datasets, including base times, forecast step frequency, grid resolution, and atmospheric variables used. Note that the wind speed components 100 metres above the surface are unavailable for the ENS model.

	HRES	ENS
Base time	00 and 12 UTC	00 and 12 UTC
Forecast step frequency	0 to 90 hours ahead by 1 93 to 144 hours ahead by 3 150 to 168 hours ahead by 6	6 hours for all forecasting horizons
Horizontal grid resolution	$0.1^\circ \times 0.1^\circ$	$0.5^\circ \times 0.5^\circ$
Atmospheric variables	10 metre zonal wind component (u_{10}) 10 metre meridional wind component (v_{10}) 100 metre zonal wind component (u_{100}) 100 metre meridional wind component (v_{100})	10 metre zonal wind component (u_{10}) 10 metre meridional wind component (v_{10}) 2 metre temperature (T_2)

Table 4: List of base times, forecast horizons, grid points and NWP variables used for weather-to-power estimation. The NWP model provides air temperature, and the zonal and meridional components of the wind speed (i.e., u_{10} and v_{10}). The variables w_{10} , d_{10} , and w_{10}^3 are estimated from u_{10} and v_{10} .

NWP base times	00 UTC and 12 UTC
Forecast horizons	Operational analysis (i.e., +0 hours ahead) and +6 hours ahead
NWP grid points	4 closest grid points to the site of interest
Direct NWP variables	10 metre zonal wind component (u_{10}) 10 metre meridional wind component (v_{10}) 2 metre temperature (T_2)
Indirect NWP variables	10 metre wind speed magnitude, $w_{10} = \sqrt{u_{10}^2 + v_{10}^2}$ 10 metre wind direction, $d_{10} = \arctan2(v_{10}, u_{10})$ Cube of 10 metre wind speed magnitude, w_{10}^3

dicted (i.e., 00, 06, 12, and 18 UTC). Continuous time series were created to overcome this by concatenating the operational analysis and shorter forecast horizon (i.e., 6-hours ahead). Table 4 presents the forecast horizons, base times, and atmospheric variables used to estimate the weather-to-power model.

The hyperparameters related to the weather-to-power model are tuned for each quantile of interest using the Bayesian Optimization algorithm with random permutation cross-validation [61]. Half of the samples are used for estimation, while the other half is used for testing. Table 5 briefly describes the hyperparameters and the search range used in hyperparameter tuning. In the case of hyperparameters not estimated through hyperparameter tuning, the adopted values are presented in Table 5.

Table 5: List of hyperparameters related to the weather-to-power model. The hyperparameter tuning was performed separately for each quantile of interest. Furthermore, they only assume integer values. The hyperparameters associated with the maximum number of features, learning rate, and subsample were not tuned.

Hyperparameter	Description	Search range or value adopted
Maximum depth	Maximum depth, limits the maximum number of nodes in a tree	[5, 9]
Minimum samples to split	Minimum number of samples required to split an internal node	[2, 350]
Minimum number of samples at a leaf	Minimum number of samples required to be at a leaf node	[2, 350]
Maximum number of features	Number of features to consider when looking for the best split	Square root of the total number of features
Learning rate	Controls the contribution of each regression tree in the additive training process	0.1
Number of estimators	Number of boosting iterations. That is, the definition of base learners in the final ensemble	[2, 150]
Subsample (or bag fraction)	Fraction of samples to be used for fitting the individual base learners	80% of the data is used for fitting the individual trees

Table 6: List of hyperparameters related to the reference method HRES-QGBT-None. The hyperparameter tuning was performed separately for each quantile and forecast horizon. Furthermore, they only assume integer values. The hyperparameters associated with the maximum number of features, learning rate, and subsample were not tuned.

Hyperparameter	Search range or value adopted
Maximum depth	[5, 9]
Minimum samples to split	[10, 160]
Minimum number of samples at a leaf	[10,110]
Maximum number of features	Square root of the total number of features
Learning rate	0.1
Number of estimators	[50, 400]
subsample	80% of the data is used for fitting the individual trees

The data samples used to estimate the methods based on the weather-to-power model are split to guarantee independence between the data used for estimating the weather-to-power modelling and ensemble combination. The first half of the samples available for model estimation is used to estimate the weather-to-power model (including the hyperparameter tuning). The second half is used to estimate the ensemble combination parameters.

The reference method HRES-QGBT-None, based on Andrade and Bessa [30], uses as input the zonal and meridional components of the wind speed provided by the deterministic NWP model at two vertical levels, i.e., 10m and 100m above the surface. Its horizontal domain comprises 5x5 NWP grid points centred on the site of interest. The number of NWP grid points used here is lower than that used by Andrade and Bessa [30]. However, the area comprised by the grid points remains the same due to the higher spatial resolution of the NWP used in Andrade and Bessa [30]. Hyperparameter tuning was performed separately for each forecast horizon and quantile. Table 6 presents the search range used in hyperparameter tuning. Table 6 presents the adopted values in the case of hyperparameters not estimated through hyperparameter tuning.

Due to the disparity between the characteristics of the ENS and HRES datasets, it is challenging to compare HRES-QGBT-None and the other studied methods. Thus, a modification of HRES-QGBT-None is included subject to constraints similar to those imposed by the TIGGE archive on the ENS dataset. This constrained version of HRES-QGBT-None is called HRES-QGBT-None. The modifications include using atmospheric variables at only one vertical level (i.e., 10 meters above the surface) and forecasting horizons with a 6-hour step frequency. Note that the horizontal grid resolution was not changed.

All GBTs used in this work were estimated using the implementation provided by Pedregosa et al. [84], and the Bayesian Optimization Algorithm used for hyperparameter tuning was provided by Head et al. [85].

3.4. Case study periods

In this work, time series are divided into two distinct sets: estimation and test. The estimation period is used to estimate the weather-to-power and ensemble calibration/combination models. In contrast, the test period is used exclusively to assess forecasting performance. No estimation or decision-making is made during this period, ensuring a clear evaluation of the forecasting models. The estimation period always comprises a time window before the testing period.

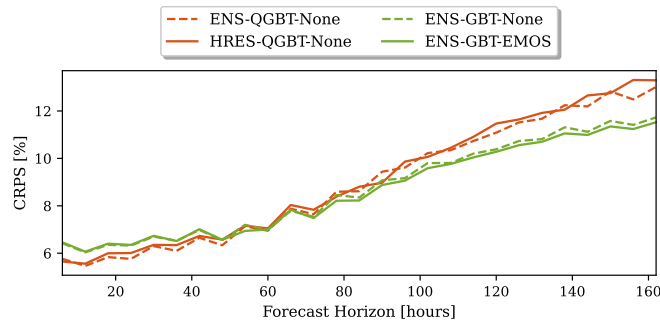
To maximise the utility of available data, we repeat the study for three distinct test periods: 2021, 2022, and 2023 with different estimation periods from 2 to 4 years, depending on data availability. The case studies are named according to the test period and estimation window. For instance, “2023-4y” refers to 2023 as the test period and the four preceding years (i.e., 2019, 2020, 2021, and 2022) as the estimation period.

4. Results and discussion

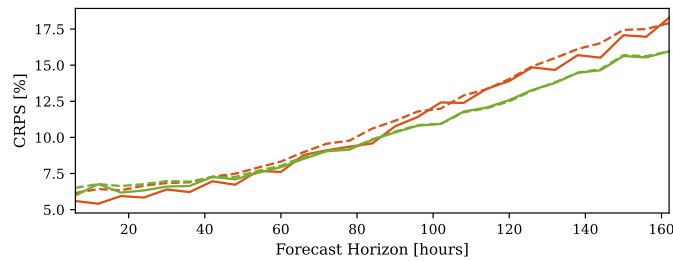
The results and discussion are divided into three subsections. The first presents the results of the reference methods based on deterministic and ensemble NWP models and discusses the added value of using ensemble NWP and the relevance of different uncertainty sources across different forecast horizons. The second presents the results related to the proposed method and compares its performance with the reference methods. The third subsection discusses forecast performance under high NWP uncertainty.

4.1. Performance of the reference methods

This work adopts four reference forecast methods introduced in Section 2.3; three based on the ensemble NWP, and one based on the deterministic NWP. The reference methods can be grouped according to how their performance degrades with increasing forecast horizons. The first group have relatively good performance for short horizons but suffers rapid degradation for longer horizons, whereas the second group perform less well for short horizons but does not degrade as much for longer horizons. Therefore, the first group, comprising HRES-QGBT-None and ENS-QGBT-None, is referred to as short-term methods, and the second comprising ENS-GBT-EMOS and ENS-GBT-None, is referred to as mid-term. Figure 3 illustrates the performance of the two groups of reference methods over the forecast horizons.



(a) Berry Burn Windfarm (BMU ID: E_BRYBW-1). Onshore farm consisting of 29 wind turbine generators, totalling a nominal capacity of 66.7 MW.



(b) London Array Windfarm Unit 4 (BMU ID: T_LARYW-4). Offshore farm consisting of 50 wind turbine generators, totalling a nominal capacity of 180 MW.

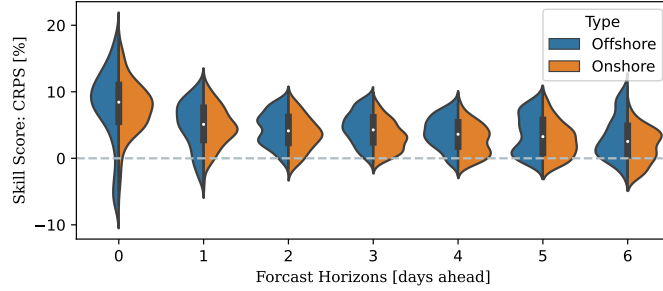
Figure 3: CRPS of the reference methods over the forecast horizons. The results presented concern the case study 2021-2y. The short-term methods are plotted in red, and the mid-term methods are in green.

Of the short-term methods, HRES-QGBT-None outperforms ENS-QGBT-

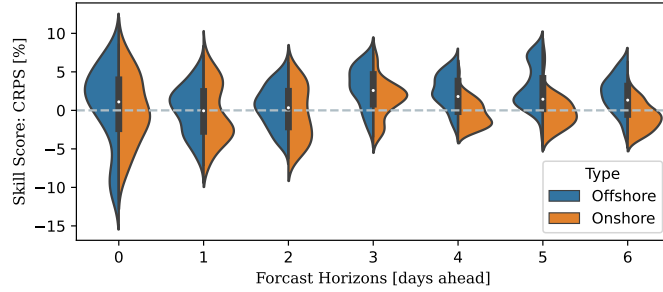
None for all forecast horizons and case studies, shown in Figure 4a. The better performance is likely due to the high temporal resolution and the larger set of atmospheric variables available from HRES compared to ENS (from TIGGE). The larger information set provides a more accurate description of the wind close to the turbine hub height, and the description of wind speed at two vertical levels enables better discrimination between atmospheric conditions by the weather-to-power model (i.e., QGBT). Moreover, the HRES model’s high temporal resolution enables the extraction of temporal features that have proven effective for achieving high performance, especially in shorter forecast horizons [30].

Figure 4(b) shows that restricting HRES-QGBT-None to the same resolution and atmospheric variables as ENS-QGBT-None, denoted HRES-QGBT-None, leads to a similar outcome for offshore wind farms, but only some onshore wind farms. Features engineered from the full-resolution deterministic NWP are more predictive than those from reduced-resolution, suggesting that all ENS-based methods presented here could be improved with access to the full-resolution model data. Due to the superior performance of HRES-QGBT-None, it will be considered the short-term forecasting reference method.

The comparison between the mid-term methods can be interpreted as performance improvement due to EMOS since both methods differ in this aspect. Figure 5 shows that the performance depends on the wind farm type. ENS-GBT-EMOS outperforms ENS-GBT-None at up to three-day-ahead horizons for offshore wind farms while narrowly underperforming for onshore wind farms. The bimodal behaviour of offshore farms in the first two days is due to a group of wind farms that benefited more from the EMOS correction. The same occurs with the onshore farms two and three days ahead. For horizons from 3 days ahead, ENS-GBT-EMOS outperforms ENS-GBT-None for onshore wind farms and obtains similar results for offshore ones. As discussed later, the weather-to-power uncertainty is more relevant than the NWP model uncertainty for short forecast horizons. However, the mid-term reference methods do not consider the weather-to-power uncertainty in the modelling process. Thus, the performance improvement due to EMOS calibration in the first horizons is mainly attributed to correcting the omission of weather-to-power uncertainty during the modelling process. On the other hand, the performance improvement in the mid-term horizons is mainly due to the correction of the ensemble spread, which improves the model’s reliability. Due to the overall performance presented by ENS-GBT-EMOS, it will



(a) CRPS skill score of HRES-QBGT-None with respect to the ENS-QBGT-None considering the case studies 2021-2y, 2022-3y and 2023-4y.



(b) CRPS skill score of HRES-QGBT-None with respect to the ENS-QBGT-None considering the case study 2021-2y.

Figure 4: CRPS skill score comparison between the short-term reference methods. Each forecast day considers the average skill score of all included forecast horizons. Figure (b) only presents the results related to the 2021-2y case study. Due to the high computational effort required, the reference method HRES-QGBT-None was estimated solely for this case study.

now be considered the mid-term forecasting reference method.

Mid-term reference methods perform better at longer forecast horizons across all wind farms and case studies. However, the horizon at which mid-term methods outperform short-term methods varies depending on the wind farm. Thus, this study examines the difference in CRPS between short- and mid-term methods over the horizons to determine when the ensemble NWP benefits forecast performance. For onshore wind farms, the mid-term method outperforms the short-term method from around four-days ahead, whereas for offshore wind farms, the mid-term method tends to outperform the short-term method from three days-ahead, and for some offshore wind farms, the mid-term method performs best for all horizons (see Figure 6).

The performance difference between short- and mid-term methods is

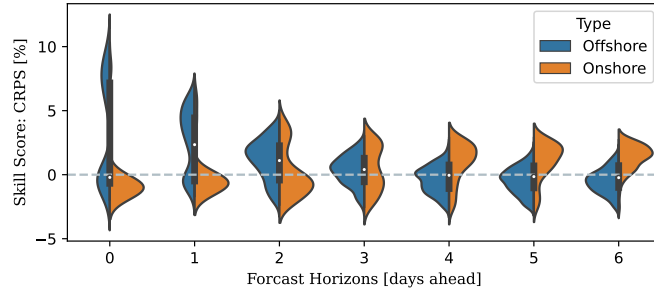


Figure 5: CRPS skill score of ENS-GBT-EMOS with respect to the ENS-GBT-None for the case studies 2021-2y, 2022-3y and 2023-4y. Each forecast day considers the average skill score of all included forecast horizons.

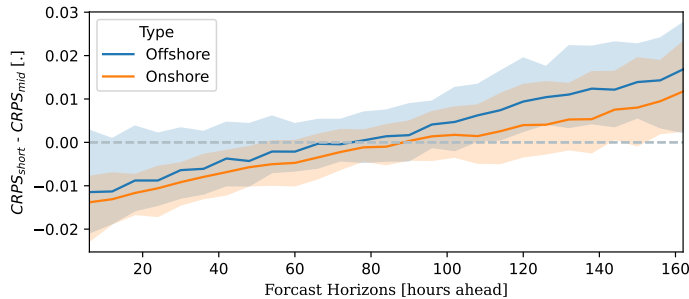
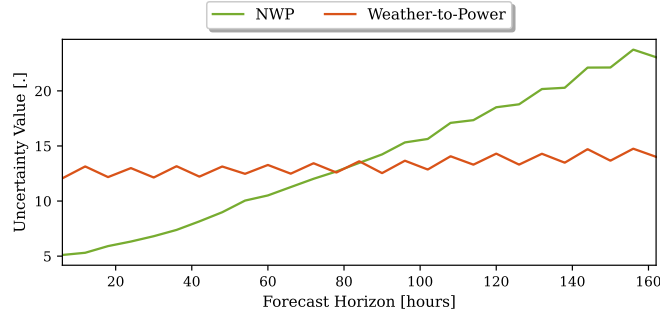


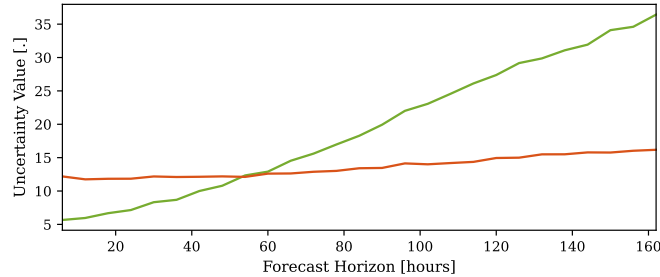
Figure 6: CRPS difference between short- and mid-term reference methods considering the 2021-2y, 2022-3y and 2023-4y case studies. Each line represents the median value, and the filled area represents the interval between the 5th and 95th percentiles.

closely related to the sources of uncertainty considered in the modelling process. Figure 7 exemplifies the relationship between forecast horizons and uncertainty values. For more information on uncertainty value, see subsection 2.3.6. NWP uncertainty increases with increasing forecast horizons. This increase is due to the inherently chaotic nature of the atmospheric system, which is well documented in the literature [86]. On the other hand, weather-to-power uncertainty presents small variability over the forecast horizons. The small variability is because weather-to-power uncertainty is affected by diurnal patterns in weather conditions.

Weather-to-power uncertainty tends to be greater than NWP uncertainty in shorter horizons, i.e., up to 48 hours ahead. Thus, forecasting methods that do not consider weather-to-power uncertainty during the modelling process have difficulty reliably forecasting these horizons. On the other hand,



(a) Berry Burn Windfarm (BMU ID: E_BRYBW-1). Onshore farm consisting of 29 wind turbine generators, totalling a nominal capacity of 66.7 MW.



(b) London Array Windfarm Unit 4 (BMU ID: T_LARYW-4). Offshore farm consisting of 50 wind turbine generators, totalling a nominal capacity of 180 MW.

Figure 7: Uncertainty value over the forecast horizons. The results presented concern the case study 2021-2y. Note that the case study and wind farms presented here are the same as those in Figure 3.

NWP uncertainty is greater for longer horizons, meaning that additional information provided by ensemble NWP has a greater impact for these horizons.

The difference between $U^{(NWP)}$ and $U^{(W2P)}$ over the forecast horizons shows dependency concerns on the farm type. However, due to the seasonality presented by $U^{(W2P)}$, it becomes difficult to analyse which horizon $U^{(NWP)}$ becomes greater than $U^{(W2P)}$. Thus, Figure 8 shows the root of the first-degree polynomial adjusted to the difference curve between $U^{(NWP)}$ and $U^{(W2P)}$. The dominance of NWP uncertainty tends to occur more frequently at shorter horizons for offshore farms than onshore ones. Thus, the relationship between the uncertainty difference and the farm type aligns with the performance difference. Therefore, the findings in Figure 8 support the dependence hypothesis between the forecasting performance and the uncer-

tainty sources considered in the modelling process.

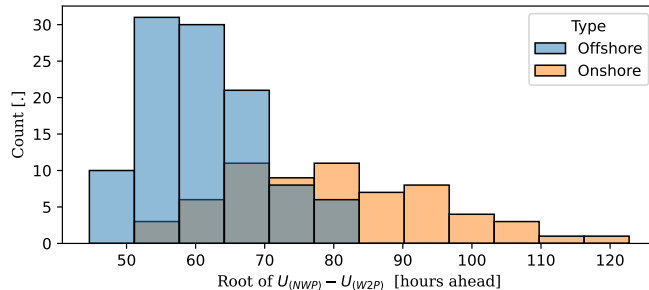


Figure 8: Histogram of the horizon at which $U^{(NWP)} = U^{(W2P)}$ by wind farm. The results present in this figure combine the 2021-2y, 2022-3y and 2023-4y case studies.

Even though the performance difference between short- and mid-term methods is linked to the type of wind farm, it shows significant variability. Thus, a seamless forecasting method capable of achieving state-of-the-art performance across all desired forecast horizons is highly valuable. However, achieving consistently state-of-the-art performance across a wide range of forecast horizons using just one predictive method is challenging as uncertainties associated with both NWP and weather-to-power must be handled effectively.

4.2. Performance of the proposed method

This study introduces a novel method to explicitly quantify and combine uncertainties related to NWP and weather-to-power. It aims to achieve state-of-the-art performance for short- and mid-term horizons (i.e., from 6 to 162 hours ahead). State-of-the-art performance is given by the reference method that achieves the best performance for a given horizon, with HRES-QBGT-None and ENS-GBT-EMOS representing short- and mid-term, respectively. The best reference method is independently chosen for each case study, wind farm, and forecast horizon based on their performance during the test period. Note that this is based on the test period results and consequently, it represents a theoretical reference that is conservative in favour of the reference methods.

Figure 9 presents the proposed method’s CRPS skill score concerning the short-term method, mid-term method, and state-of-the-art when using deterministic and ensemble NWP models with the same temporal resolution and set of atmospheric variables.

The proposed method performs similarly to the short-term reference method on the first day and outperforms it from two days-ahead. The improvement occurs for horizons in which NWP uncertainty becomes relevant. On the other hand, the proposed method outperforms the mid-term method in horizons with relevant weather-to-power uncertainty, i.e., up to one day-ahead. Consequently, the proposed method achieved state-of-the-art performance along all studied horizons.

However, the short-term reference method significantly improves accuracy when using a deterministic NWP model with higher temporal resolution and a larger set of atmospheric variables (see Figure 10). This improvement occurs because, as previously discussed, the high temporal resolution enables the extraction of temporal features that have proven effective in achieving high performance in horizons up to 48 hours ahead. Additionally, the larger set of atmospheric variables improves the classification performed by the GBT, leading to performance enhancement. Consequently, the short-term method is better than the proposed method for horizons up to the day ahead. However, despite high spatial and temporal resolution, the short-term method cannot outperform the proposed method for horizons beyond one day ahead, where weather-to-power uncertainty is relevant.

The results shown in Figure 10 indicate that the accuracy of the proposed method could be significantly enhanced by utilising the full-resolution ensemble NWP and a wider range of atmospheric variables, given that both the weather-to-power model employed by HRES-QGBT-None and the proposed method are based on GBTs. Therefore, the authors suggest investigating the performance improvement using high-resolution ensemble NWP.

The proposed method places great emphasis on the necessary computational effort. Among all the models studied in this work, the GBT used to model the weather-to-power relationship requires the most computational effort to estimate. This is attributed to the estimation of multiple GBTs and hyperparameter tuning.

The ENS-GBT-EMOS and ENS-GBT-None reference methods only require the estimation of a single GBT, regardless of the number of quantiles or forecast horizons. ENS-QGBT-None requires the estimation of one GBT for each quantile of interest, regardless of the number of forecast horizons. On the other hand, HRES-QGBT-None requires the estimation of one GBT for each quantile of interest and each forecasting horizon. However, the proposed method requires the estimation of only three GBTs, regardless of the quantiles of interest and forecast horizons (see Table 7). As a result, the

Table 7: Number of GBTs estimated for each method per wind farm for 19 quantiles of interest and 27 forecast horizons.

	Number of GBTs
ENS-GBT-None	1
ENS-QGBT-None	19
HRES-QGBT-None	513
ENS-GBT-EMOS	1
ENS-QGBT-βMM	3

proposed method achieves state-of-the-art performance while requiring low computational effort, especially when compared to HRES-QGBT-None.

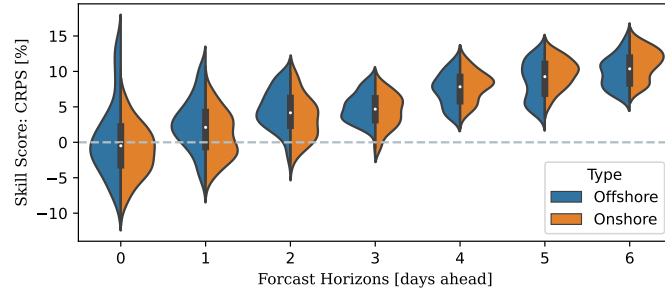
4.3. Forecasting under variable NWP uncertainty

The results presented and discussed so far originate from an overall performance assessment, as they represent average performance over multiple years. However, some events are of greater interest to decision-makers. In particular, forecasts subject to high NWP uncertainty are important. As discussed previously, NWP uncertainty tends to increase with forecast horizons due to the atmospheric system’s inherently chaotic nature. However, some atmospheric conditions are associated with high wind power forecast uncertainty, even for short horizons, such as the arrival time or precise location of a frontal system. Ensemble NWP may reflect this uncertainty through the spread of ensemble members, while deterministic NWP provides only a single weather trajectory. Figure 11 presents an example of high NWP uncertainty occurring at the relatively short lead-time of 30 hours ahead which is captured by ensemble but not deterministic NWP.

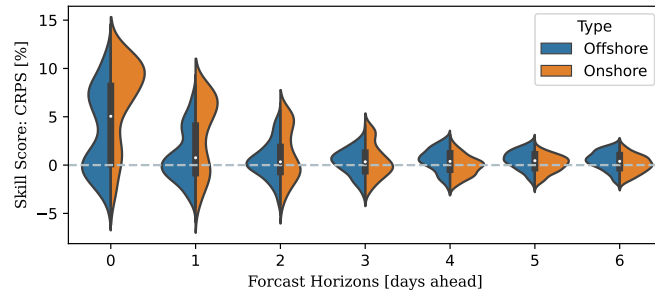
This study analyses five different scenarios. Each concerns periods in which the NWP uncertainty was greater than a given quantile of past uncertainty (i.e., inter-quartile range of wind power ensemble, see Eq. 16), calculated for each wind farm, case study, and forecast horizon. The proposed and reference methods during these periods are compared in Figure 12. When using a deterministic NWP model with the same temporal resolution and set of atmospheric variables, the proposed method outperforms the state-of-the-art at all time horizons (Figure 12). For zero and one days-ahead, an improvement compared to the state-of-the-art is present, which was not evident in the long-run average CRPS. Because the short-term reference

method does not consider the NWP uncertainty, it is not able to discriminate between high/low weather uncertainty and performance sufferers as a result.

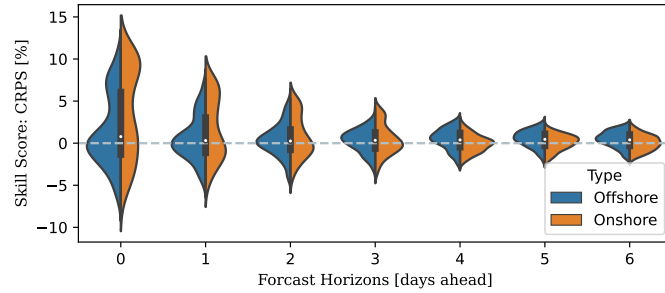
While infrequent, such events have a disproportionately large impact on decision-makers who can only take mitigating action if supplied with an informative forecast. Therefore, although it is still not considered, assessing forecast performance under high-uncertainty events should be considered in recommended practices such as IEA Wind Task 36 [87]. This highlights the significant value added by ensemble NWP that is not necessarily reflected in conventional metrics.



(a) CRPS skill score of the proposed method with respect to the HRES-QGBT-None.

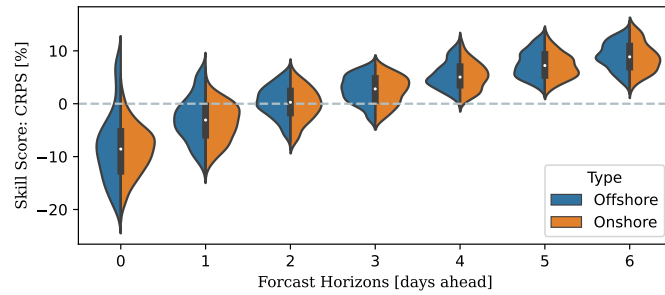


(b) CRPS skill score of the proposed method with respect to the ENS-GBT-EMOS.

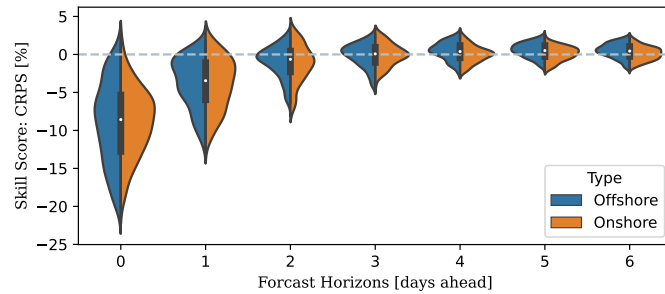


(c) CRPS skill score of the proposed method with respect to the state-of-the-art. The state-of-the-art is represented by the reference methods HRES-QGBT-None and ENS-GBT-EMOS.

Figure 9: CRPS skill score of the proposed method with respect to the short-term method, mid-term method, and state-of-the-art. The ensemble and the deterministic NWP models have the same temporal resolution and set of atmospheric variables. Note that the deterministic NWP model still has a high spatial resolution. Each forecast day considers the skill score of all included forecast horizons. This Figure presents the results related to the case study 2021-2y. Due to the high computational effort required, the reference method HRES-QGBT-None was estimated solely for this case study.

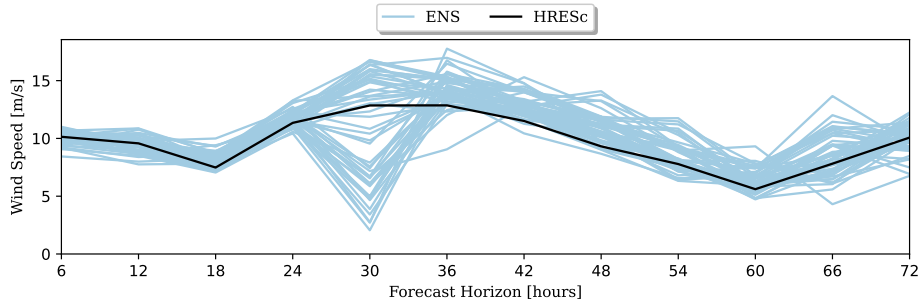


(a) CRPS skill score of the proposed method with respect to the HRES-QGBT-None.

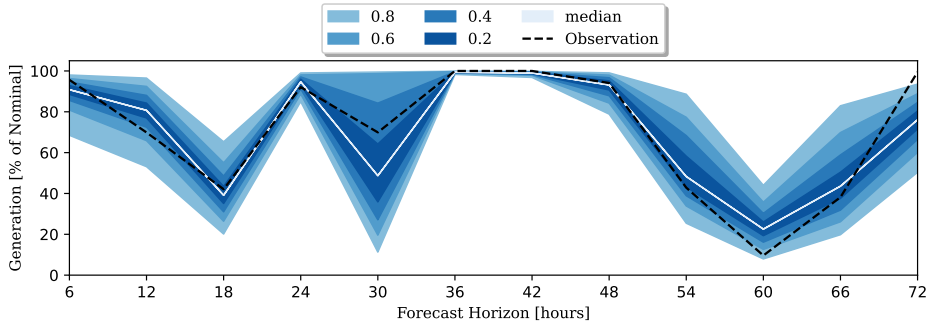


(b) CRPS skill score of the proposed method with respect to the state-of-the-art. The state-of-the-art is represented by the reference methods HRES-QGBT-None and ENS-GBT-EMOS.

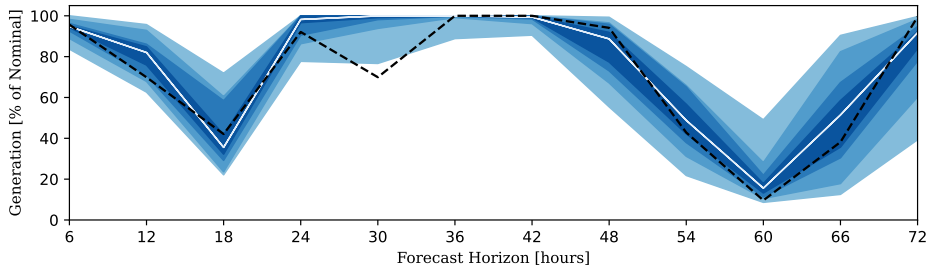
Figure 10: CRPS skill score of the proposed method with respect to the short-term method and state-of-the-art. The state-of-the-art is represented by the reference methods HRES-QGBT-None and ENS-GBT-EMOS. Each forecast day considers the average skill score of all included forecast horizons. This Figure presents the results of the case studies 2021-2y, 2022-3y and 2023-4y.



(a) Magnitude of the wind speed predicted by the ensemble (ENS) and deterministic (HRESc) NWP models



(b) Intervals predicted by ENS-QGBT-βMM



(c) Intervals predicted by HRESc-QGBT-None.

Figure 11: Example of high NWP uncertainty related to the wind farm Mocambre Offshore unit 2 (BMU ID: T_GRGBW-3) for the NWP base time 2021-12-09 00:00 and case study 2021-2y. The legend explains the colours assigned to the prediction intervals.

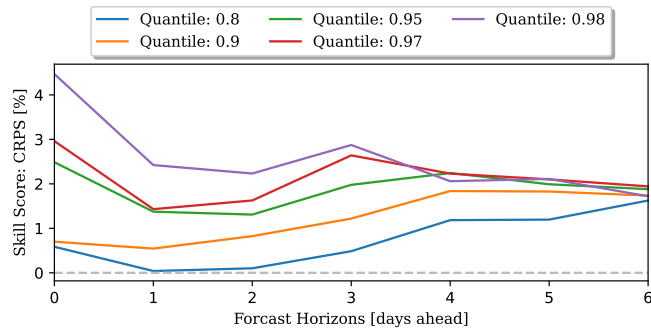


Figure 12: CRPS skill score of the proposed method with respect to the state-of-the-art under different scenarios of NWP uncertainty. The state-of-the-art is composed of the reference methods HRESc-QGBT-None and ENS-GBT-EMOS. This figure shows the results related to the case studies 2021-2y. Each scenario concerns the timestamps in which the NWP uncertainty was greater than a threshold given by a quantile. The quantile is estimated distinctly for each wind farm, case study, and forecast horizon. Each forecast day considers the skill score of all included forecast horizons. Each line represents the median of the skill score.

5. Conclusion

Wind power forecasts are subject to uncertainty originating from weather forecasts and weather-to-power conversion. This work has shown how weather-to-power uncertainty dominates short-term forecast performance, while weather forecast uncertainty dominates mid-term. Typically, the transition from one situation to the other is two- to three-days ahead, but can vary dramatically between wind farms. The transition typically occurs at shorter lead-times for offshore wind farms compared to onshore.

The method proposed here explicitly quantifies both sources of uncertainty and achieves state-of-the-art forecast performance across all horizons, where previously separate models/methods were necessary. Furthermore, performance during periods of high weather uncertainty, such as frontal passages, is improved in short-term forecasts, which state-of-the-art methods based on deterministic NWP fail to capture.

Results are based on an extensive dataset comprising 73 onshore and offshore wind farms in Great Britain over five years, i.e., from 2019 to 2023. The numerical weather forecasts are from deterministic and ensemble operational NWP models provided by the ECMWF, targeting horizons from 6 to 162 hours ahead.

The proposed method employs non-parametric uncertainty quantification for weather-to-power based on gradient-boosted quantile regression trees, which control the shape of kernels used to convert ensemble numerical weather prediction into non-parametric density forecasts of wind power production. Kernels are combined using a beta-transformed linear opinion pool to address ensemble mis-calibration and potential dependence between kernels.

Despite the encouraging results presented in this paper, the forecast method proposed here could be enhanced in several ways. First, through using a high-resolution ensemble NWP model to improve the feature engineering. Additionally, modelling the dependency between kernels instead of using opinion pools could increase the performance by allowing for non-parametric posterior distributions. Finally, performing member-by-member correction to retain spatio-temporal structure in ensemble members would allow for spatio-temporal coherence between forecasts from different wind farms.

Table 8: Zenodo repositories containing datasets and Python scripts related to this paper, including further documentation. Complete dataset exceeds 200GB. See Data Availability for terms and licences.

DOI	Repository content
10.5281/zenodo.13254469	Raw ECMWF/ HRES (from 2019 to 2021)
10.5281/zenodo.13255978	Raw ECMWF/ HRES (from 2022 to 2023)
10.5281/zenodo.13255991	Raw ECMWF/ ENS (from 2019 to 2020)
10.5281/zenodo.13256007	Raw ECMWF/ ENS (2021)
10.5281/zenodo.13256010	Raw ECMWF/ ENS (from 2022 to 2023)
10.5281/zenodo.13256014	Raw wind power production data from BMRA
10.5281/zenodo.13309890	Pre-processed BMRA data and scripts
10.5281/zenodo.13256016	Produced wind power forecasts and evaluation
10.5281/zenodo.13309948	Scripts used to produce forecasts and evaluation

Acknowledgements

Gabriel Dantas is supported by a PhD scholarship from the University of Glasgow School of Mathematics and Statistics. The authors would like to express their gratitude to the Balancing Mechanism Reporting Agent and the European Centre for Medium-Range Weather Forecasts for providing the data used in this work.

For the purpose of open access, the authors have applied a Creative Commons Attribution (CC BY) licence to any Author Accepted Manuscript version arising from this submission.

Data availability

All datasets, codes and results are available at Zenodo. Table 8 lists the repositories and their content. Contains BMRS data ©Elexon Limited copyright and database right 2024. ECMWF data is licenced under Creative Commons Attribution 4.0 International (CC BY 4.0) and is subject to ECMWF terms of use.

References

- [1] REN21, Renewables 2022: Global status report, 2022.
- [2] D. Gielen, F. Boshell, D. Saygin, M. D. Bazilian, N. Wagner, R. Gorini, The role of renewable energy in the global energy transformation, Energy Strategy Reviews 24 (2019) 38–50. doi:10.1016/j.esr.2019.01.006.

- [3] P. J. Heptonstall, R. J. K. Gross, A systematic review of the costs and impacts of integrating variable renewables into power grids, *Nature Energy* 6 (2021) 72–83. doi:10.1038/s41560-020-00695-4.
- [4] J. Petinrin, M. Shaaban, Impact of renewable generation on voltage control in distribution systems, *Renewable and Sustainable Energy Reviews* 65 (2016) 770–783. doi:10.1016/j.rser.2016.06.073.
- [5] S. Djørup, J. Z. Thellufsen, P. Sorknæs, The electricity market in a renewable energy system, *Energy* 162 (2018) 148–157. doi:10.1016/j.energy.2018.07.100.
- [6] J. Smith, S. Beuning, H. Durrwachter, E. Ela, D. Hawkins, B. Kirby, W. Lasher, J. Lowell, K. Porter, K. Schuyler, P. Sotkiewicz, Impact of variable renewable energy on us electricity markets, in: *IEEE PES General Meeting*, 2010, pp. 1–12. doi:10.1109/PES.2010.5589715.
- [7] B. Moreno, A. J. López, M. T. García-Álvarez, The electricity prices in the european union. the role of renewable energies and regulatory electric market reforms, *Energy* 48 (2012) 307–313. doi:10.1016/j.energy.2012.06.059, 6th Dubrovnik Conference on Sustainable Development of Energy Water and Environmental Systems, SDEWES 2011.
- [8] C. Sweeney, R. J. Bessa, J. Browell, P. Pinson, The future of forecasting for renewable energy, *WIREs Energy and Environment* 9 (2020) e365. doi:10.1002/wene.365.
- [9] G. Notton, M.-L. Nivet, C. Voyant, C. Paoli, C. Darras, F. Motte, A. Fouilloy, Intermittent and stochastic character of renewable energy sources: Consequences, cost of intermittence and benefit of forecasting, *Renewable and Sustainable Energy Reviews* 87 (2018) 96–105. doi:10.1016/j.rser.2018.02.007.
- [10] J. M. Morales, A. Conejo, H. Madsen, P. Pinson, M. Zugno, Integrating Renewables in Electricity Markets, volume 205 of *International Series in Operation Research & Management Sciece*, Springer, 2014.
- [11] A. Ahmed, M. Khalid, A review on the selected applications of forecasting models in renewable power systems, *Renewable and Sustainable Energy Reviews* 100 (2019) 9–21. doi:10.1016/j.rser.2018.09.046.

- [12] G. Giebel, G. Kariniotakis, 3 - wind power forecasting—a review of the state of the art, in: G. Kariniotakis (Ed.), *Renewable Energy Forecasting*, Woodhead Publishing Series in Energy, Woodhead Publishing, 2017, pp. 59–109. doi:10.1016/B978-0-08-100504-0.00003-2.
- [13] S. Han, Y. hui Qiao, J. Yan, Y. qian Liu, L. Li, Z. Wang, Mid-to-long term wind and photovoltaic power generation prediction based on copula function and long short term memory network, *Applied Energy* 239 (2019) 181–191. doi:10.1016/j.apenergy.2019.01.193.
- [14] R. J. Bessa, C. Möhrlen, V. Fundel, M. Siefert, J. Browell, S. Haglund El Gaidi, B.-M. Hodge, U. Cali, G. Kariniotakis, Towards improved understanding of the applicability of uncertainty forecasts in the electric power industry, *Energies* 10 (2017). doi:10.3390/en10091402.
- [15] R. Tawn, J. Browell, A review of very short-term wind and solar power forecasting, *Renewable and Sustainable Energy Reviews* 153 (2022) 111758. doi:10.1016/j.rser.2021.111758.
- [16] G. Giebel, C. Draxl, R. Brownsword, G. Kariniotakis, , M. Denhard, The state-of-the-art in short-term prediction of wind power. a literature overview, 2011.
- [17] C. Sweeney, R. J. Bessa, J. Browell, P. Pinson, The future of forecasting for renewable energy, *WIREs Energy and Environment* 9 (2020) e365. doi:10.1002/wene.365.
- [18] P. Bauer, A. Thorpe, G. Brunet, The quiet revolution of numerical weather prediction, *Nature* 525 (2015) 47–55. doi:10.1038/nature14956.
- [19] K. Phipps, S. Lerch, M. Andersson, R. Mikut, V. Hagenmeyer, N. Ludwig, Evaluating ensemble post-processing for wind power forecasts, *Wind Energy* 25 (2022) 1379–1405. doi:10.1002/we.2736.
- [20] S. Vannitsem, J. B. Bremnes, J. Demaeyer, G. R. Evans, J. Flowerdew, S. Hemri, S. Lerch, N. Roberts, S. Theis, A. Atencia, Z. B. Bouallègue, J. Bhend, M. Dabernig, L. D. Cruz, L. Hieta, O. Mestre, L. Moret, I. O. Plenković, M. Schmeits, M. Taillardat, J. V. den Bergh, B. V. Schaeybroeck, K. Whan, J. Ylhaisi, Statistical postprocessing for weather

- forecasts: Review, challenges, and avenues in a big data world, *Bulletin of the American Meteorological Society* 102 (2021) E681 – E699. doi:10.1175/BAMS-D-19-0308.1.
- [21] G. Casciaro, F. Ferrari, M. Cavaiola, A. Mazzino, Novel strategies of ensemble model output statistics (emos) for calibrating wind speed/power forecasts, *Energy Conversion and Management* 271 (2022) 116297. doi:10.1016/j.enconman.2022.116297.
- [22] P. Pinson, H. Madsen, Ensemble-based probabilistic forecasting at Horns Rev, *Wind Energy* 12 (2009) 137–155. doi:10.1002/we.309.
- [23] M. Lange, On the Uncertainty of Wind Power Predictions—Analysis of the Forecast Accuracy and Statistical Distribution of Errors, *Journal of Solar Energy Engineering* 127 (2005) 177–184. doi:10.1115/1.1862266.
- [24] H. Bludszuweit, J. A. Dominguez-Navarro, A. Llombart, Statistical analysis of wind power forecast error, *IEEE Transactions on Power Systems* 23 (2008) 983–991. doi:10.1109/TPWRS.2008.922526.
- [25] P. Pinson, Very-short-term probabilistic forecasting of wind power with generalized logit–normal distributions, *Journal of the Royal Statistical Society: Series C (Applied Statistics)* 61 (2012) 555–576. doi:10.1111/j.1467-9876.2011.01026.x.
- [26] J. B. Bremnes, A comparison of a few statistical models for making quantile wind power forecasts, *Wind Energy* 9 (2006) 3–11. doi:10.1002/we.182.
- [27] J. W. Messner, A. Zeileis, J. Broecker, G. J. Mayr, Probabilistic wind power forecasts with an inverse power curve transformation and censored regression, *Wind Energy* 17 (2014) 1753–1766. doi:10.1002/we.1666.
- [28] T. Hong, P. Pinson, S. Fan, H. Zareipour, A. Troccoli, R. J. Hyndman, Probabilistic energy forecasting: Global energy forecasting competition 2014 and beyond, *International Journal of Forecasting* 32 (2016) 896–913. doi:10.1016/j.ijforecast.2016.02.001.
- [29] R. Juban, H. Ohlsson, M. Maasoumy, L. Poirier, J. Z. Kolter, A multiple quantile regression approach to the wind, solar, and price tracks of

- gefcom2014, *International Journal of Forecasting* 32 (2016) 1094–1102. doi:10.1016/j.ijforecast.2015.12.002.
- [30] J. R. Andrade, R. J. Bessa, Improving renewable energy forecasting with a grid of numerical weather predictions, *IEEE Transactions on Sustainable Energy* 8 (2017) 1571–1580. doi:10.1109/TSTE.2017.2694340.
- [31] G. I. Nagy, G. Barta, S. Kazi, G. Borbély, G. Simon, Gefcom2014: Probabilistic solar and wind power forecasting using a generalized additive tree ensemble approach, *International Journal of Forecasting* 32 (2016) 1087–1093. doi:10.1016/j.ijforecast.2015.11.013.
- [32] M. Landry, T. P. Erlinger, D. Patschke, C. Varrichio, Probabilistic gradient boosting machines for GEFCom2014 wind forecasting, *International Journal of Forecasting* 32 (2016) 1061–1066. doi:10.1016/j.ijforecast.2016.02.002.
- [33] J. Guan, J. Lin, J. Guan, E. Mokaramian, A novel probabilistic short-term wind energy forecasting model based on an improved kernel density estimation, *International Journal of Hydrogen Energy* 45 (2020) 23791–23808. doi:10.1016/j.ijhydene.2020.06.209.
- [34] J. Juban, L. Fugon, G. Kariniotakis, Probabilistic short-term wind power forecasting based on kernel density estimators, in: *European Wind Energy Conference and exhibition, EWEC 2007, MILAN, Italy, 2007*, p. <http://ewec2007proceedings.info/>.
- [35] Y. Zhang, J. Wang, Gefcom2014 probabilistic solar power forecasting based on k-nearest neighbor and kernel density estimator, in: *2015 IEEE Power & Energy Society General Meeting, 2015*, pp. 1–5. doi:10.1109/PESGM.2015.7285696.
- [36] W. Dong, H. Sun, J. Tan, Z. Li, J. Zhang, H. Yang, Regional wind power probabilistic forecasting based on an improved kernel density estimation, regular vine copulas, and ensemble learning, *Energy* 238 (2022) 122045. doi:10.1016/j.energy.2021.122045.
- [37] R. J. Bessa, V. Miranda, A. Botterud, J. Wang, E. M. Constantinescu, Time adaptive conditional kernel density estimation for wind power forecasting, *IEEE Transactions on Sustainable Energy* 3 (2012) 660–669. doi:10.1109/TSTE.2012.2200302.

- [38] C. Junk, L. Delle Monache, S. Alessandrini, G. Cervone, L. Bremen, Predictor-weighting strategies for probabilistic wind power forecasting with an analog ensemble, *Meteorologische Zeitschrift* 24 (2015) 361–379. doi:10.1127/metz/2015/0659.
- [39] S. Alessandrini, L. Delle Monache, S. Sperati, J. Nissen, A novel application of an analog ensemble for short-term wind power forecasting, *Renewable Energy* 76 (2015) 768–781. doi:10.1016/j.renene.2014.11.061.
- [40] M. Shahriari, G. Cervone, L. Clemente-Harding, L. Delle Monache, Using the analog ensemble method as a proxy measurement for wind power predictability, *Renewable Energy* 146 (2020) 789–801. doi:10.1016/j.renene.2019.06.132.
- [41] E. Mangalova, O. Shesterneva, K-nearest neighbors for gefcom2014 probabilistic wind power forecasting, *International Journal of Forecasting* 32 (2016) 1067–1073. doi:10.1016/j.ijforecast.2015.11.007.
- [42] T. Miller, Explanation in artificial intelligence: Insights from the social sciences, *Artificial Intelligence* 267 (2019) 1–38. doi:10.1016/j.artint.2018.07.007.
- [43] Y.-K. Wu, P.-E. Su, T.-Y. Wu, J.-S. Hong, M. Y. Hassan, Probabilistic wind-power forecasting using weather ensemble models, *IEEE Transactions on Industry Applications* 54 (2018) 5609–5620. doi:10.1109/TIA.2018.2858183.
- [44] H. Zhang, J. Yan, Y. Liu, Y. Gao, S. Han, L. Li, Multi-source and temporal attention network for probabilistic wind power prediction, *IEEE Transactions on Sustainable Energy* 12 (2021) 2205–2218. doi:10.1109/TSTE.2021.3086851.
- [45] Y. Fujimoto, D. Nohara, Y. Kanno, M. Ohba, T. Kato, Y. Hayashi, Probability density prediction of wind farm power generation: Benchmarking natural gradient boosting approach using ensemble weather forecast, Available at SSRN 4097480 (2023). doi:http://dx.doi.org/10.2139/ssrn.4097480.

- [46] D. Kim, J. Hur, Short-term probabilistic forecasting of wind energy resources using the enhanced ensemble method, *Energy* 157 (2018) 211–226. doi:10.1016/j.energy.2018.05.157.
- [47] H. A. Nielsen, H. Madsen, T. S. Nielsen, J. Badger, G. Giebel, L. Landberg, K. Sattler, H. Feddersen, Wind power ensemble forecasting, in: *Proceedings of the 2004 Global Windpower Conference and Exhibition*, 2004.
- [48] C. Junk, L. von Bremen, D. Heinemann, Assessment of probabilistic wind power forecasts for wind farms in northern ireland, *Proceedings of the EWEA 2012 Annual Event*, Copenhagen, Denmark (2012) 16–19.
- [49] T. Gneiting, Calibration of medium-range weather forecasts, *European Centre for Medium-Range Weather Forecasts Reading*, UK, 2014.
- [50] A. E. Raftery, T. Gneiting, F. Balabdaoui, M. Polakowski, Using Bayesian Model Averaging to calibrate forecast ensembles, *Monthly Weather Review* 133 (2005) 1155 – 1174. doi:10.1175/MWR2906.1.
- [51] T. Gneiting, A. E. Raftery, A. H. Westveld, T. Goldman, Calibrated probabilistic forecasting using ensemble model output statistics and minimum crps estimation, *Monthly Weather Review* 133 (2005) 1098 – 1118. doi:10.1175/MWR2904.1.
- [52] T. Gneiting, M. Katzfuss, Probabilistic forecasting, *Annual Review of Statistics and Its Application* 1 (2014) 125–151. doi:10.1146/annurev-statistics-062713-085831.
- [53] B. Van Schaeybroeck, S. Vannitsem, Ensemble post-processing using member-by-member approaches: theoretical aspects, *Quarterly Journal of the Royal Meteorological Society* 141 (2015) 807–818. doi:10.1002/qj.2397.
- [54] A. Henzi, J. F. Ziegel, T. Gneiting, Isotonic Distributional Regression, *Journal of the Royal Statistical Society Series B: Statistical Methodology* 83 (2021) 963–993. doi:10.1111/rssb.12450.
- [55] F. Bilendo, A. Meyer, H. Badihi, N. Lu, P. Cambron, B. Jiang, Applications and modeling techniques of wind turbine power curve for wind farms - a review, *Energies* 16 (2023). doi:10.3390/en16010180.

- [56] C. Gilbert, J. Browell, D. McMillan, A hierarchical approach to probabilistic wind power forecasting, in: 2018 IEEE International Conference on Probabilistic Methods Applied to Power Systems (PMAPS), 2018, pp. 1–6. doi:10.1109/PMAPS.2018.8440571.
- [57] J. Browell, C. Gilbert, R. Tawn, L. May, Quantile combination for the EEM20 wind power forecasting competition, in: 2020 17th International Conference on the European Energy Market (EEM), 2020, pp. 1–6. doi:10.1109/EEM49802.2020.9221942.
- [58] J. H. Friedman, Greedy function approximation: A gradient boosting machine, *The Annals of Statistics* 29 (2001) 1189–1232.
- [59] G. Ke, Q. Meng, T. Finley, T. Wang, W. Chen, W. Ma, Q. Ye, T.-Y. Liu, Lightgbm: A highly efficient gradient boosting decision tree, in: I. Guyon, U. V. Luxburg, S. Bengio, H. Wallach, R. Fergus, S. Vishwanathan, R. Garnett (Eds.), *Advances in Neural Information Processing Systems*, volume 30, Curran Associates, Inc., 2017.
- [60] T. Chen, C. Guestrin, Xgboost: A scalable tree boosting system, in: *Proceedings of the 22nd ACM SIGKDD International Conference on Knowledge Discovery and Data Mining, KDD '16*, Association for Computing Machinery, New York, NY, USA, 2016, p. 785–794. doi:10.1145/2939672.2939785.
- [61] J. Snoek, H. Larochelle, R. P. Adams, Practical bayesian optimization of machine learning algorithms, in: F. Pereira, C. Burges, L. Bottou, K. Weinberger (Eds.), *Advances in Neural Information Processing Systems*, volume 25, Curran Associates, Inc., 2012.
- [62] V. Chernozhukov, I. Fernández-Val, A. Galichon, Quantile and probability curves without crossing, *Econometrica* 78 (2010) 1093–1125. doi:10.3982/ECTA7880.
- [63] F. Zhou, J. Wang, X. Feng, Non-crossing quantile regression for distributional reinforcement learning, in: H. Larochelle, M. Ranzato, R. Hadsell, M. Balcan, H. Lin (Eds.), *Advances in Neural Information Processing Systems*, volume 33, Curran Associates, Inc., 2020, pp. 15909–15919.
- [64] T. Gneiting, R. Ranjan, Combining predictive distributions, *Electronic Journal of Statistics* 7 (2013) 1747 – 1782. doi:10.1214/13-EJS823.

- [65] T. Gneiting, A. E. Raftery, Strictly proper scoring rules, prediction, and estimation, *Journal of the American statistical Association* 102 (2007) 359–378.
- [66] T. Gneiting, F. Balabdaoui, A. E. Raftery, Probabilistic Forecasts, Calibration and Sharpness, *Journal of the Royal Statistical Society Series B: Statistical Methodology* 69 (2007) 243–268. doi:10.1111/j.1467-9868.2007.00587.x.
- [67] J. Browell, S. Haglund, H. Kälvegren, E. Simioni, R. Bessa, Y. Wang, D. van der Meer, Hybrid energy forecasting and trading competition, 2023. doi:10.21227/5hn0-8091.
- [68] M. Scheuerer, D. Möller, Probabilistic wind speed forecasting on a grid based on ensemble model output statistics, *The Annals of Applied Statistics* 9 (2015) 1328 – 1349. doi:10.1214/15-A0AS843.
- [69] M. A. Matos, R. J. Bessa, C. Gonçalves, L. Cavalcante, V. Miranda, N. Machado, P. Marques, F. Matos, Setting the maximum import net transfer capacity under extreme res integration scenarios, in: *2016 International Conference on Probabilistic Methods Applied to Power Systems (PMAPS)*, 2016, pp. 1–7. doi:10.1109/PMAPS.2016.7764145.
- [70] P. Pinson, H. Madsen, H. A. Nielsen, G. Papaefthymiou, B. Klöckl, From probabilistic forecasts to statistical scenarios of short-term wind power production, *Wind Energy* 12 (2009) 51–62. doi:10.1002/we.284.
- [71] M. A. Matos, R. J. Bessa, Setting the operating reserve using probabilistic wind power forecasts, *IEEE Transactions on Power Systems* 26 (2011) 594–603. doi:10.1109/TPWRS.2010.2065818.
- [72] C. Gonçalves, L. Cavalcante, M. Brito, R. J. Bessa, J. Gama, Forecasting conditional extreme quantiles for wind energy, *Electric Power Systems Research* 190 (2021) 106636. doi:10.1016/j.epsr.2020.106636.
- [73] J. Beirlant, I. F. Alves, T. Reynkens, Fitting tails affected by truncation, *Electronic Journal of Statistics* 11 (2017) 2026 – 2065. doi:10.1214/17-EJS1286.

- [74] A. J. McNeil, T. Saladin, The peaks over thresholds method for estimating high quantiles of loss distributions, in: Proceedings of 28th international ASTIN Colloquium, volume 23, 1997, p. 43.
- [75] F. N. Fritsch, J. Butland, A method for constructing local monotone piecewise cubic interpolants, *SIAM Journal on Scientific and Statistical Computing* 5 (1984) 300–304. doi:10.1137/0905021.
- [76] J. W. Messner, P. Pinson, J. Browell, M. B. Bjerregård, I. Schicker, Evaluation of wind power forecasts—an up-to-date view, *Wind Energy* 23 (2020) 1461–1481. doi:10.1002/we.2497.
- [77] S. Arnold, E.-M. Walz, J. Ziegel, T. Gneiting, Decompositions of the mean continuous ranked probability score, arXiv preprint arXiv:2311.14122 (2023).
- [78] S. Bentzien, P. Friederichs, Decomposition and graphical portrayal of the quantile score, *Quarterly Journal of the Royal Meteorological Society* 140 (2014) 1924–1934. doi:10.1002/qj.2284.
- [79] P. Pinson, P. McSharry, H. Madsen, Reliability diagrams for non-parametric density forecasts of continuous variables: Accounting for serial correlation, *Quarterly Journal of the Royal Meteorological Society* 136 (2010) 77–90. doi:10.1002/qj.559.
- [80] Elexon, Balancing mechanism reporting agent, 2024. URL: <https://bscdocs.elexon.co.uk/service-descriptions/balancing-mechanism-reporting-agent-service-description>, accessed: 2024-05-06.
- [81] National Grid Electricity System Operator Limited, The grid code, <https://dcm.nationalgrideso.com/>, 2024. Issue 6.
- [82] J. Yan, C. Möhrle, T. Göçmen, M. Kelly, A. Wessel, G. Giebel, Uncovering wind power forecasting uncertainty sources and their propagation through the whole modelling chain, *Renewable and Sustainable Energy Reviews* 165 (2022) 112519. doi:10.1016/j.rser.2022.112519.
- [83] J. Yan, H. Zhang, Y. Liu, S. Han, L. Li, Uncertainty estimation for wind energy conversion by probabilistic wind turbine power curve modelling,

Applied Energy 239 (2019) 1356–1370. doi:10.1016/j.apenergy.2019.01.180.

- [84] F. Pedregosa, G. Varoquaux, A. Gramfort, V. Michel, B. Thirion, O. Grisel, M. Blondel, P. Prettenhofer, R. Weiss, V. Dubourg, J. Vanderplas, A. Passos, D. Cournapeau, M. Brucher, M. Perrot, E. Duchesnay, Scikit-learn: Machine learning in Python, *Journal of Machine Learning Research* 12 (2011) 2825–2830.
- [85] T. Head, M. Kumar, H. Nahrstaedt, G. Louppe, I. Shcherbatyi, scikit-optimize/scikit-optimize, 2021. doi:10.5281/zenodo.5565057.
- [86] R. Buizza, M. Milleer, T. N. Palmer, Stochastic representation of model uncertainties in the ecmwf ensemble prediction system, *Quarterly Journal of the Royal Meteorological Society* 125 (1999) 2887–2908. doi:10.1002/qj.49712556006.
- [87] IEA Wind Task 36, Recommended practices for selecting renewable power forecasting solutions, <https://iea-wind.org/task51/task51-publications/task51-recommended-practices/>, 2019.